ChemPubSoc Europe

DOI: 10.1002/ejoc.201701538

EurJOC European Journal of Organic Chemistry

Full Paper

Azolotriazines | *Very Important Paper* |

VIP

Thermal Ring-Opening of Pyrazolo[3,4-*d*][1,2,3]triazin-4-ones: An Experimental and Theoretical Study

Juan P. Colomer,[a][‡] María L. Sciú,[a][‡] Cristina L. Ramirez,[b] Silvia M. Soria-Castro,[a] D. Mariano A. Vera,*[b] and Elizabeth L. Moyano*[a]

Abstract: Several 3-pyrazolylcarbonyl-pyrazolo[3,4-*d*][1,2,3]triazin-4-ones have been prepared from 5-amino-1*H*-pyrazole-4-carbonitriles through a simple sequence. In the first step, diazotization of the corresponding aminopyrazoles afforded pyrazolo[3,4-*d*][1,2,3]triazin-4-ones. Next, thermal rearrangement of these compounds through nitrogen elimination gave the final products. The proposed mechanism for the ring-opening of the pyrazolotriazinones to give the pyrazolylcarbonyl-pyrazolotriazinones involves the generation of an iminoketene intermediate, which reacts with a second molecule of pyrazolotriazinone. The complete mechanism of product formation involving the iminoketene intermediate, and all other reasonable pathways, have been explored in detail through DFT calculations. Furthermore, additional experiments to corroborate the presence of the iminoketene intermediate were carried out.

Introduction

Many structural analogues of the naturally occurring purine bases have attracted attention due to their broad spectrum of biological activity.[1] In particular, azole-annulated 1,2,3-triazines possess activity as anti-virals and anti-tubercular agents, inhibitors of protoporphyrinogen oxidase, herbicides, and pesticides, among others.[2–4] In view of the important biological activities of purine analogues, our research interests have been focused on the synthesis of pyrazolo[3,4-*d*][1,2,3]triazin-4-ones and imidazo[4,5-*d*][1,2,3]triazin-4-ones, establishing a convenient method to access a broad range of these derivatives through the one-pot diazotization of 5-aminoazole-4-carbonitrile precursors.[5,6] We found that the stability and transformations of the diazonium ion intermediate was strongly dependent on the type of azole ring and, to a lesser extent, the nature of the substituent at N-1.[6]

Concerning the chemical reactivity of azole-annulated 1,2,3-triazinones, it has been found that modifications at the carbonyl group lead to 4-substituted azolo-triazines,[2,4,7] alkylation at N-3[8] and opening of the triazine ring with elimination of nitrogen afford pyrazole derivatives[9–12] or pyrazolyl-pyrazolo-oxazinones by the dimerization of an iminoketene intermediate.[11,12] However, the study of nitrogen-loss reactions of azolotriazines as an approach to preparing new heterocycles has not been so widely explored, despite the synthetic potential of the precursors.

Following our studies of azolotriazine compounds, we report here the thermally induced elimination of nitrogen from pyrazolo[3,4-*d*][1,2,3]triazin-4-ones to give 3-(pyrazolylcarbonyl)-pyrazolotriazinones by a simple protocol. A mechanism for the formation of the new pyrazolotriazinone amides is proposed based on a detailed exploration of the complex potential energy surfaces of all reasonable pathways using first-principles quantum chemical calculations. Also, a novel microwave-assisted preparation of the aminopyrazole precursors of pyrazolo[3,4-*d*][1,2,3]triazin-4-ones is described.

Results and Discussion

First, 5-amino-1*H*-pyrazole-4-carbonitriles **3a**–**g**, as precursors of pyrazolotriazinones **4a**–**g**, were synthesized by applying focused microwave irradiation. As background information to the application of the microwave methodology, the flow microwave synthesis of this type of aminopyrazoles in very good yields should be mentioned.[13] In our approach, compounds **3a**–**g** were prepared from ethoxymethylenemalononitrile (**1**) and hydrazines (**2**) using ethanol as solvent at a temperature of 100 °C and 300 W irradiation for 2–7 minutes (Scheme 1). The addition of triethylamine as base was required for the neutralization of the acid salts of the hydrazines. According to the results, in several cases, the application of microwaves improved the pyrazole yields in comparison with conventional synthesis; however, the main advantage was the significant reduction of the reaction times from hours to minutes (Table 1).[5,6] In particular, for the synthesis of **3b**, the use of a mixture of water and ethanol as solvent led to an improved yield; it was found that

[a] *INFIQC, Department of Organic Chemistry, School of Chemical Sciences, National University of Córdoba, Córdoba, Argentine*
E-mail: lauramoy@fcq.unc.edu.ar
http://infiqc.fcq.unc.edu.ar
[b] *QUIAMM-INBIOTEC, Dept. of Chemistry, School of Exact and Natural Sciences, National University of Mar del Plata, Mar del Plata, Argentine*
E-mail: dmavera@yahoo.com
http://inbiotec-conicet.gob.ar/investigacion/quiamm-area/
[‡] These authors contributed equally to this publication.
Supporting information and ORCID(s) from the author(s) for this article are available on the WWW under https://doi.org/10.1002/ejoc.201701538.

the optimum ratio of water/ethanol was 1:3 (v/v). When the amount of water was increased, the yield decreased. In the case of the reaction in equal amounts of the two solvents, the yield of **3b** diminished to 59 %, and when only water was used the yield of pyrazole was only 20 %.

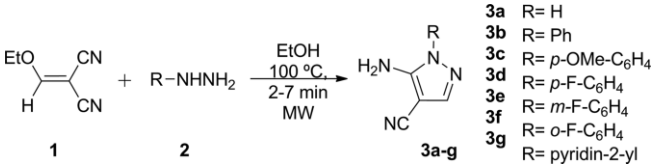

Scheme 1. Microwave-assisted synthesis of 5-amino-1*H*-pyrazole-4-carbonitriles **3a**–**g**.

Table 1. Synthesis of 5-amino-1*H*-pyrazole-4-carbonitriles **3a**–**g** by conventional and microwave-assisted methodologies.

Compound	R	Yield (%)	
		Conventional[a]	Microwave[b]
3a	H	45	69
3b	Ph	63	67 (74,[c] 88[d])
3c	*p*-OMe-C_6H_4	69	72
3d	*p*-F-C_6H_4	97	79
3e	*m*-F-C_6H_4	51	74
3f	*o*-F-C_6H_4	91	81
3g	Pyridin-2-yl	27	48

[a] EtOH reflux, $N(Et)_3$, time: 2–6 h. Isolated yields. [b] EtOH, $N(Et)_3$, 100 °C, time: 2–7 min, 300 W. [c] EtOH/H_2O (2:1. v/v), 100 °C, time: 2 min, 300 W. [d] EtOH/H_2O (3:1. v/v), 100 °C, time: 2 min, 300 W.

Next, compounds **3a**–**g** were subjected to diazotization conditions to prepare pyrazolo[3,4-*d*][1,2,3]triazin-4-ones **4a**–**g** using the protocol previously described (Scheme 2).[5,6] The yields of compounds **4** were good, with the exception of the pyridinyl derivative **4g** and the 7-unsubstituted pyrazolotriazinone **4a**, the latter reaction proving totally unsuccessful (Table 2). In the case of **4g**, the depleted yield can be attributed to difficulties in the purification of this product from the reaction mixture. The unsuccessful conversion of **3a** into **4a** could be explained by the lower stability of the diazo group in the pyrazole-diazonium intermediate, which prevents the formation of the triazinone ring. It is known that the reactivity and stability of the diazonium cation is strongly dependent on its substituents;

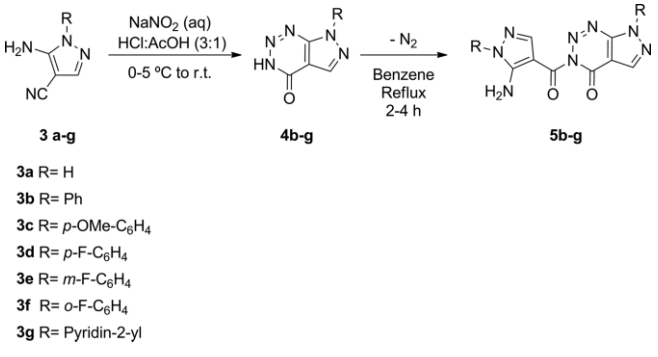

Scheme 2. Synthesis of pyrazolotriazinones **4** and **5** from aminopyrazoles **3**.

electron-withdrawing groups generally increase the electrophilic properties of the diazo group whereas electron-donating substituents stabilize the diazonium cation reducing the electrophilicity of the diazo group.[14] In the case of the cyclization reaction to form the triazinone ring, the diazonium cation should be electrophilic and stable enough to attack the nitrile group, minimizing other competitive reactions.

Table 2. Synthesis of pyrazolotriazinones **4b**–**g** and **5b**–**g**.

R	Compd.	Yield (%)[a]	Compd.	Yield (%)[a]
H	**4a**	–	–	–
Ph	**4b**	77	**5b**	67
p-OMe-C_6H_4	**4c**	88	**5c**	46
p-F-C_6H_4	**4d**	70	**5d**	62
m-F-C_6H_4	**4e**	52	**5e**	51
o-F-C_6H_4	**4f**	64	**5f**	66
Pyridin-2-yl	**4g**	39	**5g**	g[b]

[a] Isolated yields. [b] Determined by ^1H NMR spectroscopy.

The structures of the 3*H*-pyrazolotriazinone tautomers **4b**–**g** were confirmed by NMR and IR spectroscopy, and the spectral data gave good agreement with those previously reported.[5,6,10]

The thermal treatment of compounds **4b**–**g** in benzene at reflux afforded the new compounds 3-(5-aminopyrazol-4-ylcarbonyl)pyrazolotriazinones **5b**–**g**. Regarding the reactivities of the different triazinones **4** with respect to the formation of compounds **5**, it is noticeable that the pyridinyl precursor (**4g**) did not react to give product **5g** in any considerable amount (only 9 %). This result indicates that the feasibility of triazine ring-opening strongly depends on the substitution at N-7 in the pyrazole moiety. In this sense, stabilization of the triazine ring could be achieved when a pyridinyl group is present in the fused pyrazole ring.

The identities of these new pyrazolotriazinones **5** were unambiguously confirmed by NMR and IR spectroscopy as well as by high-resolution mass spectrometry. For example, the ^1H NMR spectrum of **5b** shows the presence of a characteristic singlet for the pyrazole 13-H proton (δ = 7.74 ppm), a typical singlet for the triazine 5-H proton (δ = 8.54 ppm), and a broad signal for the amino protons (δ = 6.94 ppm; Figure 1). Also, a characteristic doublet for the *ortho* aromatic protons of the phenyl group attached to N-7 in the triazine ring was assigned (δ = 8.19 ppm). Analysis of the ^{13}C NMR spectra and 2D experiments allowed the assignment of the two carbonylic carbons, one be-

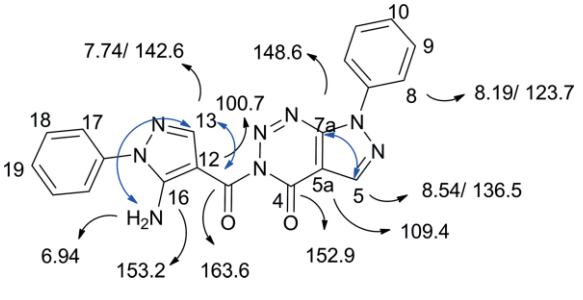

Figure 1. NMR spectroscopic data for **5b**: Assignment of the main protons and carbons as well as the correlations.

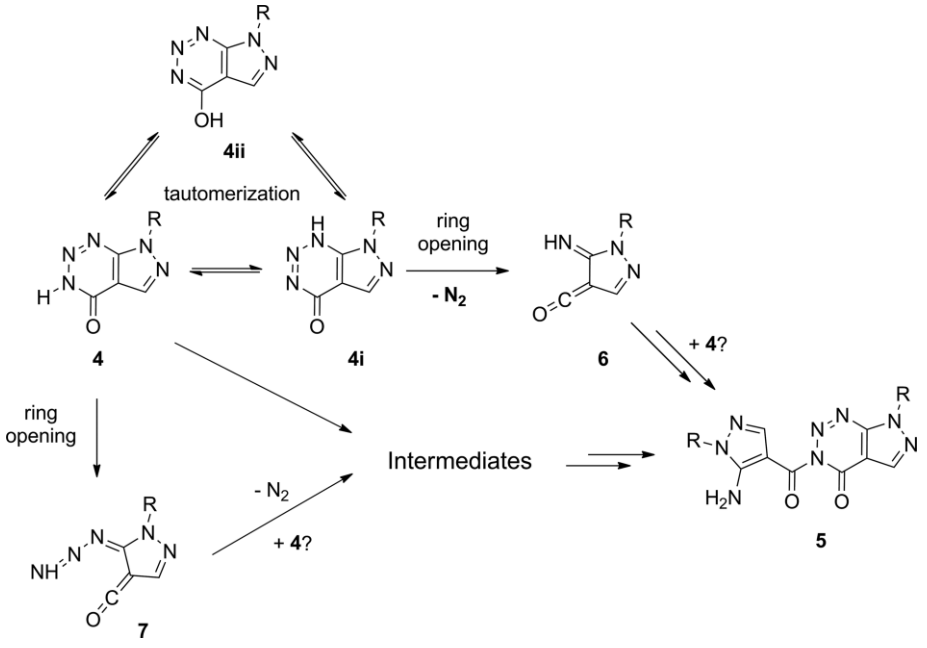

Scheme 3. Possible reaction pathways to the formation of pyrazolotriazinones **5**.

longs to the triazinone ring (δ = 152.9 ppm) and the other links the triazine to the pyrazole ring (δ = 163.6 ppm), and the olefinic carbons C-16 (δ = 153.2 ppm), C-5 (δ = 136.5 ppm), C-13 (δ = 142.6 ppm), C-5a (δ = 109.4 ppm), C-7a (δ = 148.6 ppm), and C-12 (δ = 100.7 ppm; see Figure 1). In addition, the IR spectrum shows two bands corresponding to the stretching of the two C=O bonds at 1716 and 1692 cm^{-1} and a typical N–H stretching vibration at 3461 cm^{-1}.

To explore the formation of **5**, different pathways were considered. The proposed mechanism for the formation of pyrazolylcarbonyl-pyrazolotriazinones **5b**–**g** is depicted in Scheme 3.

The formation of compounds **5b**–**g** is likely analogous to the thermal conversion of 1,2,3-benzotriazin-4(3*H*)-one into anthraniloyl-benzotriazinone, through the elimination of molecular nitrogen, ultimately leading to quinazolino[3,2-*c*][1,2,3]-benzotriazin-8-one.[15,16] It should be mentioned that the anthraniloyl-benzotriazinone (analogue of the pyrazolylcarbonyl-pyrazolotriazinones described here) was not isolated and for this reason was postulated as an intermediate in that reaction. Subsequently, the intermediate could undergo a cyclodehydration reaction in diethylene glycol dimethyl ether at reflux to give the quinazolino-fused derivative.

Pyrazolotriazinone **4** could undergo nitrogen extrusion by a retro-Diels–Alder reaction, as was proposed for the thermolysis of pyrrolotriazines **9**, or following ring-opening, as was proposed for the photochemical reactions of benzotriazinones.[17] Elimination of nitrogen from **4** could lead to the imidoylketene **6** or even an azetinone intermediate, which can coexist in equilibrium.[15,18–22] These intermediates could react with a nucleophile, in this case a second molecule of **4** or a better suited tautomer of it, to give the final product **5**. Similar nucleophilic reactions have previously been reported for benzoazetinones to give aminobenzamides and anthranilate esters.[23]

Alternatively, pyrazolotriazinone **4**, either intact or after ring-opening, may undergo nucleophilic addition at the amide carbonyl group by another pyrazolotriazinone molecule. The ring-opening of polycyclic 1,2,3-triazines with nucleophiles has been described in the literature, the triazinone suffering nucleophilic attack at the exposed and reactive C-4 position by a further molecule of triazinone.[15,16,24] In particular, in the thermolysis of 1,2,3-benzotriazin-4-one, an unstable aryl-triazene intermediate was postulated to form in the ring-opening reaction before leading to the *o*-aminobenzoyl derivatives.[15]

In addition, the reaction of pyrazolotriazinones **4** (via the iminoketene or by direct nucleophilic attack) to form pyrazolylcarbonyl-triazinones **5** was favored over the simple dimerization of iminoketenes to give oxazinone derivatives as previously observed in the thermolysis of pyrrolediones,[25] benzotriazinones,[15] and pyrazolotriazinones.[11] In this last work, phosphorus pentoxide was required for the thermal transformation of the triazinones into pyrazolo-oxazinones.

According to the literature on the thermolysis of pyrazolotriazinone analogues, different mechanisms would arise depending mainly on when the nitrogen molecule is released and the possibility of the formation of the iminoketene **6**.

In view of the mechanistic scope for obtaining **5** from **4**, all reasonable mechanistic pathways (in terms of free energy) were considered in a detailed ab initio exploration of the free-energy surfaces. Five main possibilities will be discussed and are labeled as paths A–E (Scheme 4). The computational procedure was carried out at the CAM-B3LYP/6-311+G(d,p) level of theory, the efficacy of which was successfully proved in a related heterocyclic mechanistic study.[22] The potential energy surface study was performed for the formation of compounds **5b** (R = Ph) and **5c** (R = *p*-MeO-C_6H_4), taken as representatives. Additionally, energy calculations at the MP2, MP3, and MP4(DQ)/6-

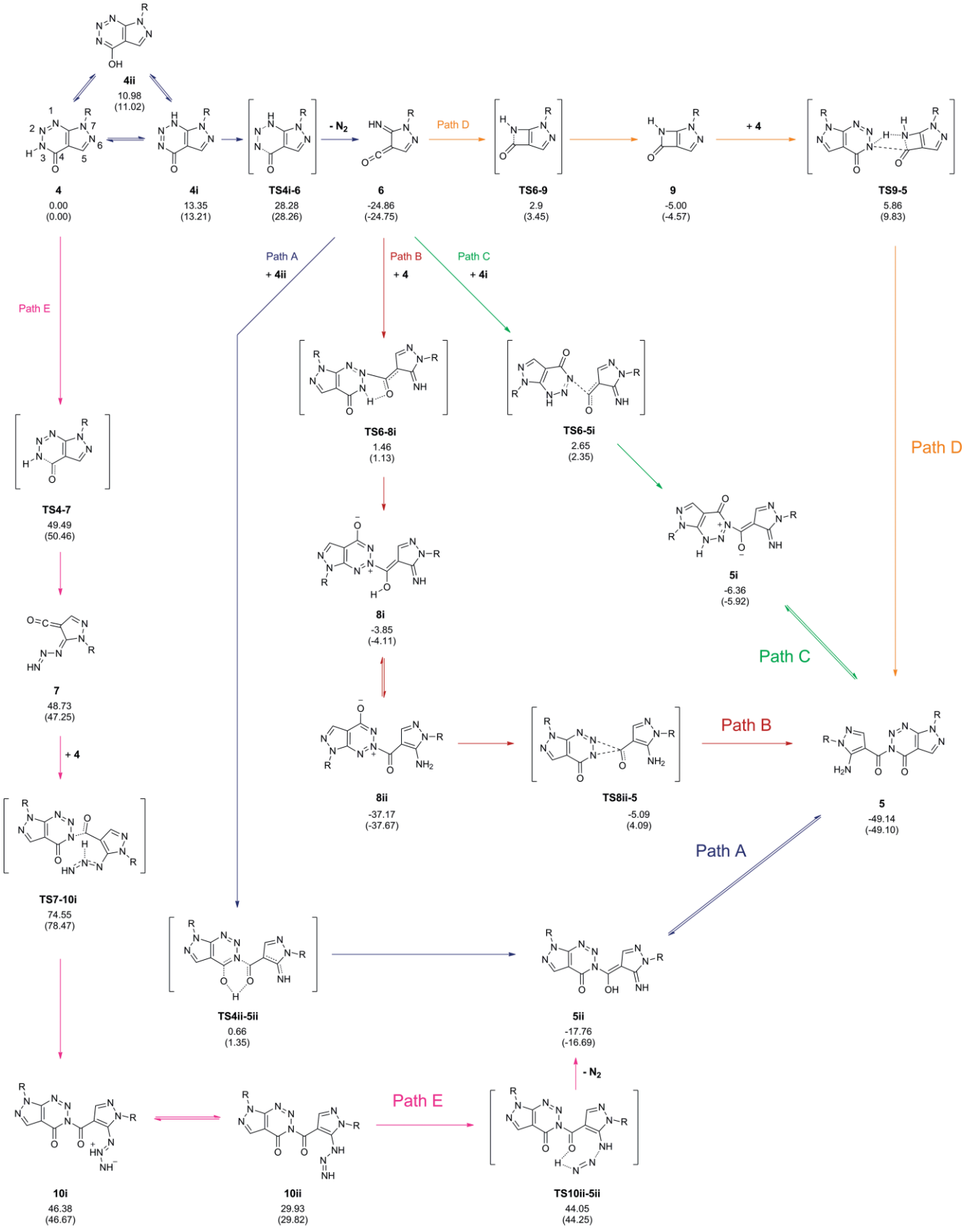

Scheme 4. Summary of the computational mechanistic study. Relative standard free energies below each structure label are indicated for the different mechanistic pathways for **4b** → **5b** (and for **4c** → **5c** in parentheses). All energies (in kcal/mol) are given relative to the energy of 2 equivalents of the reactants **4b** and **4c**.

311+G(d,p) levels were carried out for all stationary points found for the derivative **5b** (see Table S2 in the Supporting Information). In Scheme 4, the relative standard free energies at 298.15 K of all the stationary points are shown below the corresponding structure for R = Ph and in parentheses for R = *p*-MeO-C_6H_4. The relative free energies are given with respect to the corresponding reactants **4b** and **4c**.

First, of the three different tautomers of **4** (**4**, **4i**, and **4ii**), only **4i** (13.3 and 13.2 kcal/mol above **4b** and **4c**, respectively) would be able to productively release N_2 at the beginning of the process. Hereafter, no further attention will be paid to the interconversion of tautomers, because fast tautomeric equilibria are expected under the reaction conditions. Indeed, the double proton transfer (DPT) for **4** to another molecule of itself or another intermediate would be one of the possible mechanisms for tautomer interconversion. Bovarets' et al. have extensively studied this kind of DPT in DNA base pairs and found interconversion barriers between 8 and 13 kcal/mol for thymine tautomerization assisted by another thymine (canonical and enol pair) and for guanine-thymine pairs (canonical pair to enol pair), respectively.[26,27] These values are considerably lower than the energies required for the proposed reaction pathways from **4**, as shown later (either 28.5 or 49.5 kcal/mol through the different pathways).

The relative free energies of the transition state for early nitrogen release, **TS4i-6b**/**TS4i-6c**, were found to be practically the same in both cases (28.3 kcal/mol) and led to the iminoketene intermediate **6b/c**, which is considerably stable (–24.9 and –24.8 kcal/mol, respectively; see the structure of **TS4i-6b**, as a representative, in Figure 2).

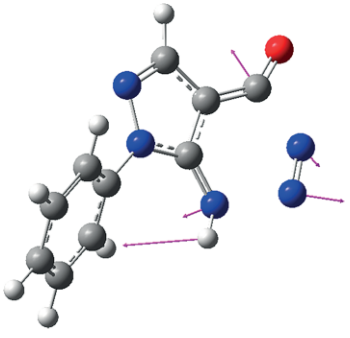

Figure 2. Structure of the transition state **TS4i-6b** for the concerted release of nitrogen from **4ib**. Vectors indicate the imaginary frequency *xyz* displacement vectors.

This earlier nitrogen release is the initial step of four mechanistic variants (paths A–D) that are based on the intermediacy of iminoketene **6**. As can be noted by inspecting its molecular electrostatic potential (Figure 3), intermediate **6** proves to be a very strong electrophile, and can attack either a nucleophilic nitrogen in the triazine ring of a second molecule of **4** (or one of its tautomers) or, intramolecularly, its own imino nitrogen.

In paths A and B, the attack of iminoketene **6** at a nucleophilic nitrogen of the triazine ring of **4** (or one of its tautomers) is considered. Of these, the direct reaction of **6** with a molecule of **4** to form a new C–N bond between the ketene carbon and

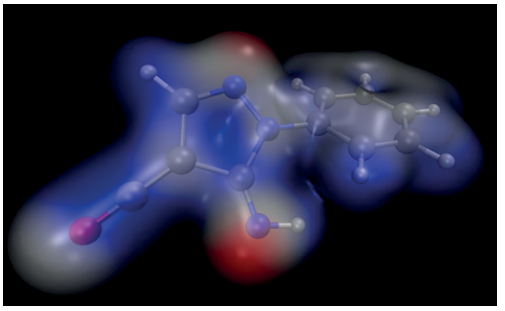

Figure 3. Molecular electrostatic potential of **6b** colored from red (–0.1 a.u.) to blue (+0.1 a.u.) on an isodensity surface (electron density of 0.01 a.u.).

N-3 of **4** can clearly be disregarded, because this nitrogen is not at all nucleophilic (N-3 is signaled by a yellow arrow in Figure 4); essentially N-2 and N-1 are much more nucleophilic than N-3, as can be noted by inspection of the electrostatic potential of **4c** in Figure 4. Thus, an encounter with **4** will lead to coupling of the ketene carbon with one of the other nitrogen atoms; as shown later, the lowest-energy transition state for an encounter with **4** involves coupling with N-2.

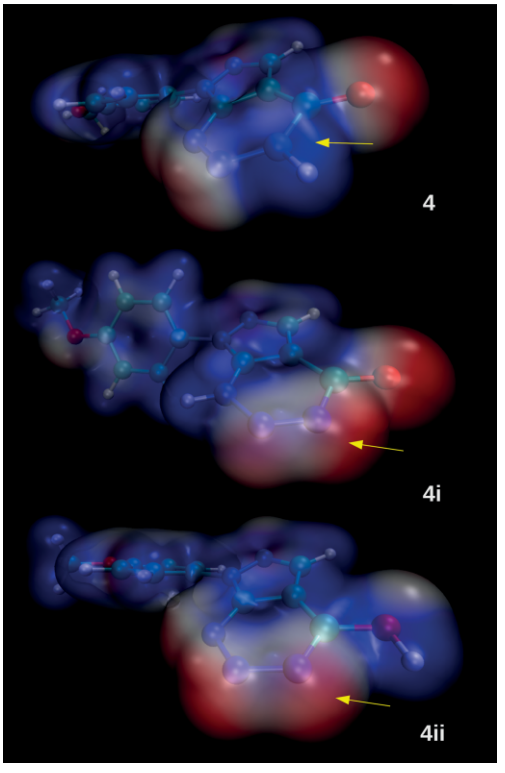

Figure 4. Molecular electrostatic potentials for the tautomers postulated to react with **6c**: **4c**, **4ic**,and **4iic** as representatives (similar charge distribution for **4b**, **4ib**, and **4iib**). The nitrogen forming the C–N bond in the final product **5c** (N-3) is indicated by a yellow arrow. It appears to be slightly electrophilic in **4c** and a fine nucleophile in the cases of both **4ic** and **4iic**. In the case of **4iic**, despite the similar colors for N-3 and N-2, N-3 is the most nucleophilic with an ESP charge of –0.615 compared with –0.560 on N-2 (a similar pattern was found for **4iib** with –0.598 on N-3 and –0.539 on N-2). Colors and scale as in Figure 3.

In the cases of **6b** or **6c**, path A proceeds by an encounter with a molecule of the tautomer **4ii** passing through the transi-

tion state **TS4ii-5ii** (shown in Figure S1 in the Supporting Information) to give **5ii**, which is a tautomer of the final product **5** (Scheme 4). This TS has the lowest energy of the four possible alternatives paths A–D available for **6** in the case of the phenyl derivative (0.66 kcal/mol of relative free energy) and the second lowest energy in the case of the anisyl derivative (1.35 kcal/mol).

Along path B, **6** reacts directly with **4** to generate a new C–N bond with the N-2 of the triazine ring, passing through **TS6-8ib**/**c** (at a relative free energy of 1.46 and 1.13 kcal/mol, respectively) to yield the intermediate **8i**, which readily tautomerizes to **8ii**, the most stable intermediate. Then **8ii** isomerizes via a three-membered-ring TS, **TS8ii-5**, which leads to the final product **5**. The transition state **TS8ii-5b** is notably lower in energy (by 9.0 kcal/mol) than its counterpart **TS8ii-5c** (see Figure 5). In this case the effect of the electron-donating group changes the electron distribution in the π systems of both the pyrazole and triazine rings. In this way, **TS8ii-5c** exhibits stronger bonding character, thereby making it harder to rearrange than **TS8ii-5b**, as confirmed through the natural bond order (NBO) analysis depicted in Figure S2 in the Supporting Information, in which the Wiberg bond orders are summarized for the two TSs.

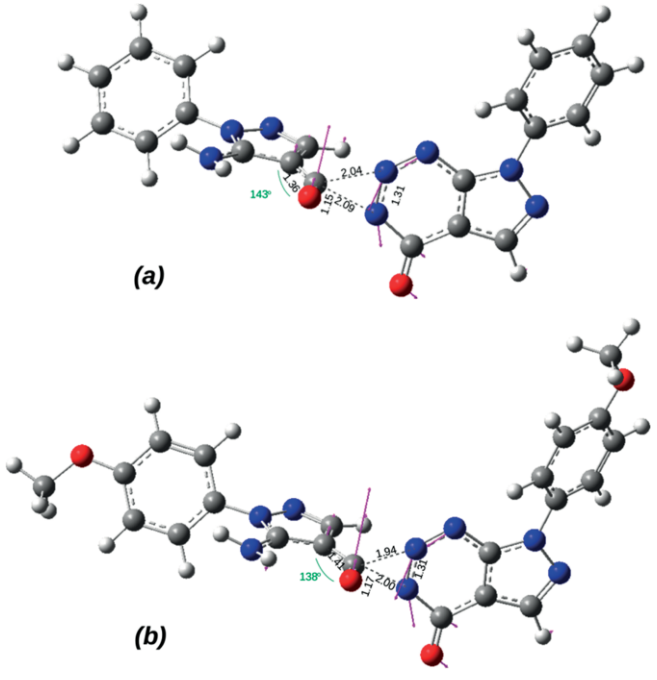

Figure 5. Structures and main geometrical features of the TSs for the N-2→N-3 rearrangement to give the products **5b** and **5c** through path B: a) **TS8ii-5b** and b) **TS8ii-5c**. Vectors indicate the imaginary frequency *xyz* displacement vectors.

Direct coupling of the ketene electrophile with N-3 of the triazine to directly yield **5** is also possible with the tautomer **4i** through path C (Scheme 4). As shown in Figure 4, the N-3 of **4ic** (yellow arrow) is the most nucleophilic nitrogen and it will readily couple to the ketene C of **6c**. This is similar to the case of **4iic**, in contrast to what was found for **4c**, in which N-3 seems to be electrophilic. Thus, the third possible intermolecular reaction of **6** is the encounter with the tautomer **4i** of the reactant, as depicted in the path C (Scheme 4). The encounter complex formed between **6** and **4i** yields the intermediate **5i**, passing through the transition state **TS6-5i** with a relative energy of about 2.5 kcal/mol (similar for R = Ph and *p*-MeO-C_6H_4). This TS has a relative energy slightly higher than either **TS6-8i** or **TS4ii-5ii** (between 1 and 2.5 kcal/mol above those for the reaction of **6** + **4ii** through path A and **6** + **4** through path B, respectively). However, **5i** still has a relatively high free energy and, once formed, it readily tautomerizes to the final product **5** without the irreversible formation of the stable isomer **8ii**, as in the case of path B.

In path D the isomerization of **6** to the fused azetinone intermediate **9** is considered through intramolecular attack of the ketene C on the imine N. Intermediate **9** could directly attack N-3 of **4**, because it initiates adduct formation by transferring its proton, turning N-3 nucleophilic as it approaches the amide carbonyl group. The transition state **TS9-5**, with relative free energies of 5.9 and 9.8 kcal/mol for **9b** and **9c**, respectively, finally leads to the final product **5** (see Figure S4 in the Supporting Information). In this case the electron densities of the two different substituents have a small effect on the energies (ca. 4 kcal/mol).

All the paths discussed so far start with an early release of the nitrogen molecule. However, different possibilities can be considered for a later N_2 release. One of these, with the lowest free energy, is labeled as path E. However, this path would be extremely unlikely in comparison with the alternatives involving an earlier N_2 release and the intermediacy of iminoketene **6** (paths A–D). The different free-energy profiles for path A–E are compared in Figure 6 for R = Ph and in Figure 7 for R = *p*-MeO-C_6H_4.

Along path E, **4** would first undergo ring-opening (alone or concerted with association with another molecule of **4**, not shown) to form **7**, a ketene nucleophile with retention of all the nitrogen atoms of the broken triazine. Ketene **7** then couples with **4** to give adduct **10i**. Next, this adduct tautomerizes to **10ii** and finally releases a molecule of N_2 to yield the intermediate **5ii**, a tautomer of the product **5**. It should be noted than all the TSs and even the most stable intermediate within path E have higher free energies than the free energy of the highest TS in the pathways based on an early release of N_2 (paths A–D, Scheme 4, Figure 6, and Figure 7).

Comparison of the reaction profiles in Figure 6 and Figure 7 reveals that the phenyl and anisyl derivatives follow very similar pathways, always passing through the iminoketene key intermediate **6**. However, the possibility of controlling the kinetics after the irreversible formation of the isomer **8ii** seems more likely to happen in the **4c** → **5c** reaction, as shown in the previous discussion and Figure 5.

Next, we performed several experiments to clarify the reaction mechanism and verify the presence of the reaction intermediates. First, thermolysis of **4b** was carried out in a mixture of benzene/water as solvent (Scheme 5). It is known that ketenes like **6** in the presence of water easily form carboxylic

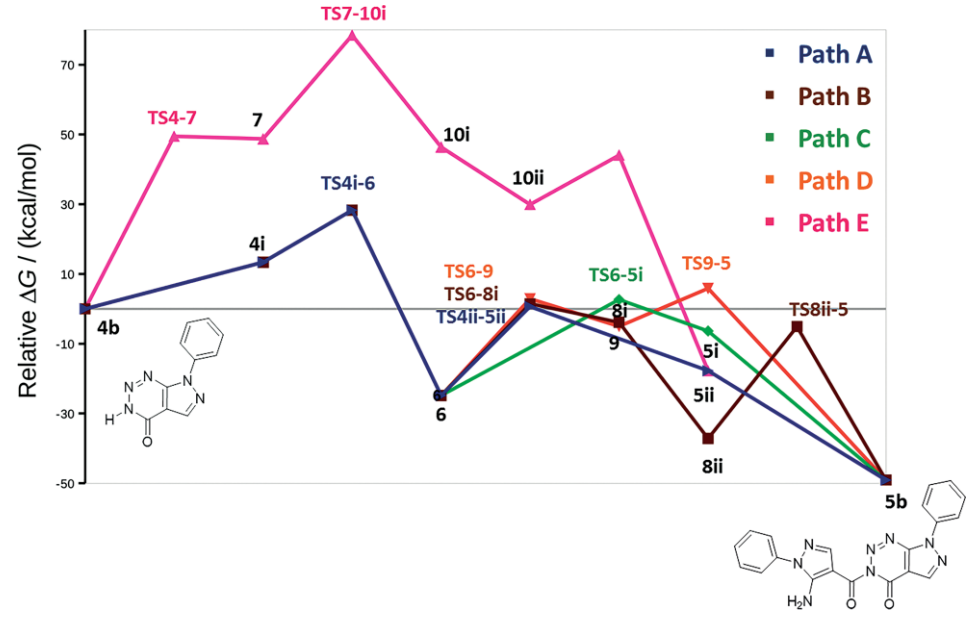

Figure 6. Free-energy profiles for the mechanistic pathways for the **4b** → **5b** reaction. Color codes correspond to paths A–E, as shown in Scheme 4.

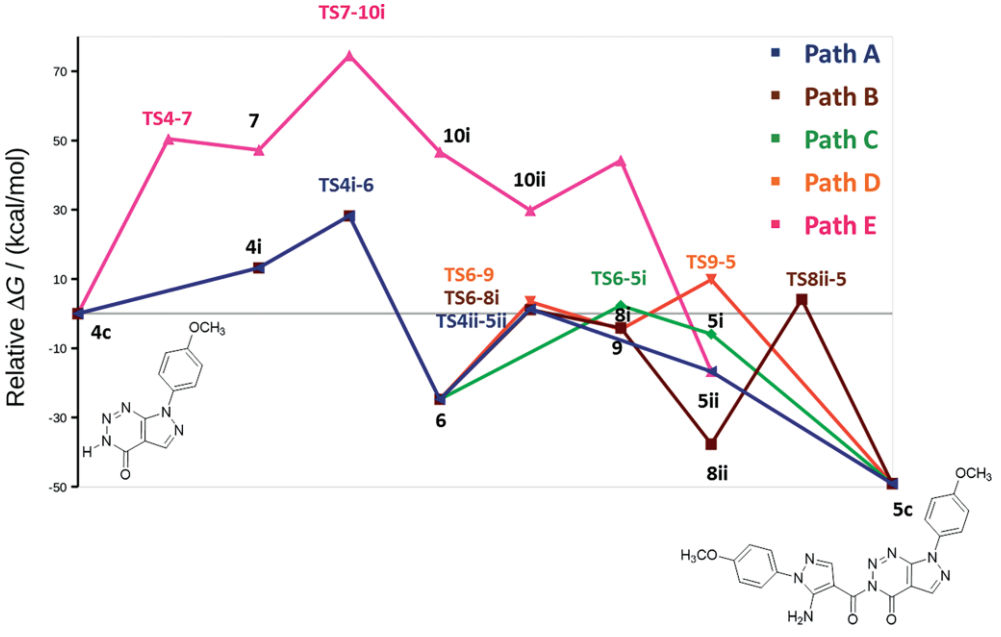

Figure 7. Free-energy profiles for the mechanistic pathways for the **4c** → **5c** reaction. Color codes correspond to Paths A–E, as shown in Scheme 4.

acids.[19] Analysis of the reaction mixture showed the presence of the amino acid derivative **11** (63 % yield) and the aminopyrazole **12** (11 % yield). The formation of **12** can be rationalized by decarboxylation of **11** during the thermolysis over several hours.[28]

On the other hand, it has been reported that the chlorination of pyrazolotriazinones with phosphorus oxychloride gives pyrazole-4-carbonyl chlorides[11] by reaction of the iminoketene intermediate with the chlorinating agent. When we treated **4b** with catalytic amounts of $SOCl_2$ and DMF at reflux, the pyrazole-4-carboxylic acid **11** was isolated as the main product (52 % yield) instead of the pyrazole-4-carbonyl chloride, which surely hydrolyzes under the reaction conditions.

To confirm the importance of nucleophilic species in the reaction, the nitrogen elimination reaction of pyrazolotriazinone **4b** was carried out in the presence of two amino compounds, *p*-toluidine and aminopyrazole **3b**. Reaction with toluidine afforded amide **13** in 59 % yield, whereas the reaction with **3b** led to the attractive *N*-pyrazolylpyrazolecarboxamide **14** (59 % yield). Pyrazolotriazinone **5b** was not detected in any of the reaction mixtures. These findings support that the intermediates formed from **4b** react with other nucleophilic species

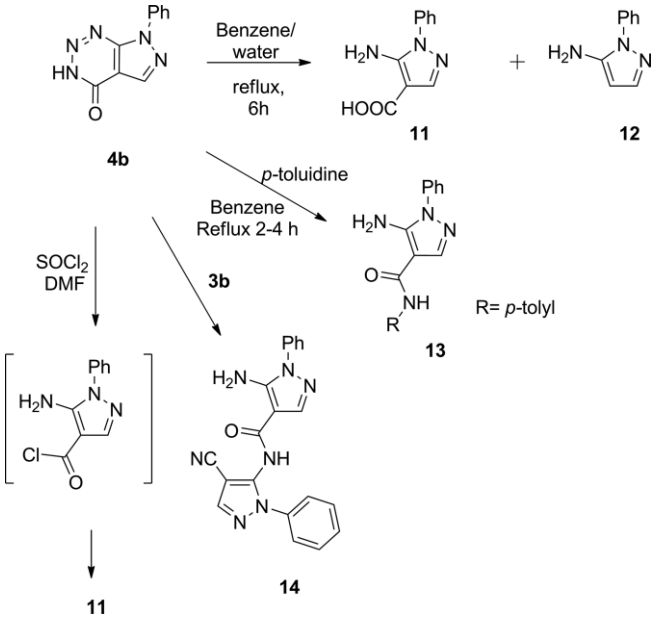

Scheme 5. Reactions of pyrazolotriazinone **4b** under different conditions.

(amines or water) faster than with another triazinone **4b** to give amides or acid products.

Conclusions

A novel thermal transformation of 7-aryl/heteroarylpyrazolo-[3,4-*d*][1,2,3]triazin-4-ones has been studied. The combination of one molecule of pyrazolotriazinone and the iminoketene produced by nitrogen elimination from another molecule of pyrazolotriazinone could explain the formation of the attractive 3-(pyrazolylcarbonyl)-pyrazolotriazinone derivatives. In this case the ketene undergoes nucleophilic substitution by N-3 of the triazinone moiety to form the amide product. The reaction was successful with 7-aryl-substituted pyrazolotriazines, whereas the pyridinyl derivative was almost unreactive, perhaps because of the stability of the triazinone ring, with respect to the nitrogen extrusion reaction.

A mechanistic study undoubtedly ruled out the possibility of nitrogen molecule release at any stage other than the very first step of the mechanism (**TS4i-6**, Scheme 4 and Figure 2), leading to iminoketene intermediate **6**. The iminoketene was found to be the key intermediate in four reasonable pathways, all of them with TS and intermediate energies less than the energy of **TS4i-6**. Once **6** is formed, it can either isomerize to the azetinone **9** before coupling with the reactant **4** (path D) or directly react with **4** (path B) or one of its tautomers, either **4i** (path C) or **4ii** (path A). The fate of the phenyl derivative would clearly be rate-controlled by the release of N_2 following the preferred path A. Similar behavior would be expected for the anisyl derivative, except that in this case, once **6c** is formed the smaller barrier to subsequent reaction lies in path B, which involves an irreversible reaction that produces an isomer of the final product, which slowly isomerizes.

In agreement with calculations, the reaction of phenyl derivative **4b** would endorse the formation of iminoketene intermediate **6** in the ring-opening of triazinone, similarly to previously described reactions of benzotriazinones.

The synthesis of amides like **5**, **13**, or **14** through the application of this simple methodology opens a range of possibilities for obtaining heterocyclic amides containing both pyrazolyl and pyrazolotriazinyl substituents.

Experimental Section

General: All reagents obtained from commercial sources were used without further purification. Microwave experiments were carried out in a CEM-Discovery Labmate monomode microwave oven. NMR spectra were recorded with a 400 MHz Bruker spectrometer (^{1}H at 400.16 MHz and ^{13}C at 100.62 MHz) at ambient temperature. Solutions were typically prepared in either $CDCl_3$, $(CD_3)_2CO$, or [D_6]DMSO with the chemical shifts referenced to deuteriated solvent as internal standard. The ^{1}H NMR spectroscopic data are reported as follows: Chemical shift (δ), multiplicity (s, singlet; d, doublet; t, triplet; q, quartet; m, multiplet; br., broad; dd, doublet of doublets, etc.), coupling constant (J) in Hz, and integration (e.g., 1 H). HRMS was performed by using the electrospray ionization (ESI) technique and Q-TOF detection. FTIR spectra were recorded by using a Nicolet iN10 spectrometer (Thermo Scientific, USA) with an MCT (mercury cadmium telluride) detector and Ominc Picta workstation. Spectra were collected by acquiring 64 scans in high-resolution (8 cm^{-1}) mode.

General Procedure for the Synthesis of 5-Amino-1*H*-pyrazole-4-carbonitriles 3a–g: Ethoxymethylenemalononitrile (**1**; 0.122 g, 1 mmol) was added to a mixture of hydrazine **2** (1.2 mmol) in ethanol (2 mL) and heated using microwave irradiation (300 W) for 2–7 minutes at 100 °C in a closed system. To obtain compound **3a** the hydrazine sulfate salt was used, whereas for compounds **3b**–**g** hydrazine hydrochloride was employed. In the case of **3b** and **3g**, the solid obtained was isolated by filtration and washed with cold water. Prior to the reaction with malononitrile **1**, neutralization of hydrazine salts was carried out with an equimolar amount of triethylamine. For compounds **3a** and **3c**–**f**, the residue was extracted with chloroform (3 × 5 mL) and dried with anhydrous $MgSO_4$. The resulting solution was concentrated to dryness and the solid was recrystallized from ethanol, isolated by filtration, and washed with cold ethanol. The spectral data of compounds **3a**–**d**,**f** correspond to literature data.[5,6,29]

5-Amino-1-(3-fluorophenyl)-1*H*-pyrazole-4-carbonitrile (3e): This compound was obtained as a yellow solid in 74 % yield (149 mg). ^{1}H NMR [400 MHz, $(CD_3)_2CO$, 25 °C]: δ = 7.71 (s, 1 H, 3-H), 7.60 (td, J = 8.2, 6.5 Hz, 1 H, 12-H), 7.46 (ddd, J = 8.1, 1.7, 0.8 Hz, 1 H, 13-H), 7.40 (br. dt, J = 9.8, 2.1 Hz, 1 H, 9-H), 7.23 (tdd, J = 8.6, 2.5, 0.9 Hz, 1 H, 11-H), 6.25 (br. s, 2 H, 7-H) ppm. ^{13}C NMR [101 MHz, $(CD_3)_2SO$, 25 °C]: δ = 163.7 (d, J = 245.8 Hz, C-10), 152.2 (C-5), 142.5 (C-3), 140.3 (d, J = 10.2 Hz, C-8), 132.1 (d, J = 9.2 Hz, C-12), 120.9 (d, J = 3.1 Hz, C-13), 115.7 (d, J = 21.2 Hz, C-11), 114.4 (C-6), 112.4 (d, J = 25.0 Hz, C-9), 76.1 (C-4) ppm.

5-Amino-1-(pyridin-2-yl)-1*H*-pyrazole-4-carbonitrile (3g): This compound was obtained as a yellow solid in 48 % yield (88 mg). ^{1}H NMR [400 MHz, $(CD_3)_2SO$, 25 °C]: δ = 8.47 (ddd, J = 4.9, 1.7, 0.7 Hz, 1 H, 10-H), 8.11 (br. s, 2 H, 7-H), 8.02 (ddd, J = 8.5, 7.4, 1.9 Hz, 1 H, 12-H), 7.89 (s, 1 H, 2-H), 7.85 (br. d, J = 8.4 Hz, 1 H, 13-H), 7.35 (ddd, J = 7.4, 5.0, 1.0 Hz, 1 H, 11-H) ppm. ^{13}C NMR [101 MHz, $(CD_3)_2SO$, 25 °C]: δ = 153.2 (C-8), 153.0 (C-5), 147.1 (C-10), 142.5 (C-3), 139.9 (C-12), 121.2 (C-11), 114.4 (C-6), 113.3 (C-13), 73.3 (C-4) ppm.

General Procedure for the Synthesis of Pyrazolo[3,4-*d*][1,2,3]triazin-4-ones 4b–g: Aqueous $NaNO_2$ (0.124 g, 1.8 mmol, 1 mL) was added to a stirred and cooled solution (0–5 °C) of pyrazole **3** (1 mmol) in a mixture of HCl/AcOH (3:1, 20 mL) over a period of 10 min. The reaction mixture was then warmed to room temperature and stirred for 20 h. The resulting precipitate of pyrazolotriazinone was filtered off and the residue was diluted with water (20 mL), extracted with dichloromethane (3 × 30 mL), and dried with anhydrous $MgSO_4$. The resulting solution was concentrated to dryness and the solid was then purified by column chromatography with dichloromethane and dichloromethane/ethyl acetate in different proportions as eluent. The spectral data of compounds **4b**–**d**,**f** correspond to literature data.[5,6]

7-(3-Fluorophenyl)-4*H*-pyrazolo[3,4-*d*][1,2,3]triazin-4-one (4e): ***((<=Author: For 4e and 4g, insert '3,7-dihydro' into the name?))*** This compound was obtained as a white powder in 52 % yield (120 mg). ^{1}H NMR [400 MHz, $(CD_3)_2SO$, 25 °C]: δ = 15.39 (s, 1 H, 5-H), 8.65 (s, 1 H, 3-H), 8.00–7.93 (m, 2 H, 8-H, 12-H), 7.70 (dt, *J* = 8.3, 6.6 Hz, 1 H, 11-H), 7.38 (tdd, *J* = 8.5, 2.5, 0.8 Hz, 1 H, 10-H) ppm. ^{13}C NMR [101 MHz, $(CD_3)_2SO$, 25 °C]: δ = 162.1 (d, *J* = 244.5 Hz, C-9), 153.7 (C-4), 148.3 (C-7a), 138.8 (d, *J* = 10.7 Hz, C-13), 135.8 (C-3), 131.5 (d, *J* = 9.1 Hz, C-11), 118.3 (d, *J* = 3.0 Hz, C-12), 115.1 (d, *J* = 20.9 Hz, C-10), 109.7 (d, *J* = 26.6 Hz, C-8), 108.1 (C-3a) ppm. HRMS (ESI$^+$): calcd. for $C_{10}H_7N_5OFH^+$ 232.06291; found 232.06279.

7-(Pyridin-2-yl)-4*H*-pyrazolo[3,4-*d*][1,2,3]triazin-4-one (4g): This compound was obtained as yellow crystals in 39 % yield (83 mg). ^{1}H NMR [400 MHz, $(CD_3)_2SO$, 25 °C]: δ = 8.64 (ddd, *J* = 4.8, 1.8, 0.7 Hz, 1 H, 9-H), 8.49 (s, 1 H, 3-H), 8.14 (td, *J* = 7.6, 1.9 Hz, 1 H, 10-H), 7.82 (dt, *J* = 8.2, 0.8 Hz, 1 H, 12-H), 7.63 (ddd, *J* = 7.5, 4.8, 1.0 Hz, 1 H, 11-H) ppm. ^{13}C NMR [101 MHz, $(CD_3)_2SO$, 25 °C]: δ = 149.7 (C-4), 148.6 (C-9), 143.4 (C-3), 139.9 (C-10), 133.4 (C-7a), 125.0 (C-11), 119.0 (C-12), 111.7 (C-13), 94.4 (C-3a) ppm.

General Procedure for the Synthesis of 3-(5-Aminopyrazol-4-ylcarbonyl)pyrazolo[3,4-*d*][1,2,3]triazin-4-ones 5b–g: Benzene (10 mL) was added to pyrazolotriazines **4** (0.25 mmol) and the mixture was stirred and heated at reflux for 2–6 h. The solvent was then evaporated and the solid obtained was purified by column chromatography with dichloromethane/ethyl acetate in different proportions as eluent.

3-(5-Amino-1-phenyl-1*H*-pyrazol-4-ylcarbonyl)-7-phenyl-3,7-dihydro-4*H*-pyrazolo[3,4-*d*][1,2,3]triazin-4-one (5b): This compound was obtained as a white solid in 67 % yield (66 mg). M.p. 189.2 °C (decomp.). ^{1}H NMR [400 MHz, $(CD_3)_2CO$, 25 °C]: δ = 8.54 (s, 1 H, 3-H), 8.20–8.17 (m, 2 H, 8-H, 12-H), 7.74 (s, 1 H, 3′-H), 7.71–7.64 (m, 4 H, 9-H, 11-H, 8′-H, 12′-H), 7.61–7.54 (m, 3 H, 10-H, 9′-H, 11′-H), 7.48 (tt, *J* = 7.3, 1.3 Hz, 1 H, 10′-H), 6.94 (s, 2 H, 5′-H) ppm. ^{13}C NMR [101 MHz, $(CD_3)_2CO$, 25 °C]: δ = 163.6 (C-6′), 153.2 (C-5′), 152.9 (C-4), 148.6 (C-7a), 142.6 (C-3′), 138.9 (C-13), 138.3 (C-7′), 136.5 (C-3), 130.6 (C-9′, C-11′), 130.4 (C-9, C-11), 129.4 (C-10), 129.3 (C-10′), 125.2 (C-8′, C-12′), 123.7 (C-8, C-12), 109.4 (C-3a), 100.7 (C-4′) ppm. FTIR (KBr): $\tilde{\nu}$ = 3434.83 (νN–H), 1712.84 (νC=O ketone), 1686.35(νC=O amide), 1609.81(νC=C aromatic) cm^{-1}. MS (EI): *m/z* (%) = 399 (7) [M + 1]$^+$, 398 (8) [M]$^+$, 370 (30), 328 (12), 213 (45), 186 (77), 156 (11), 91 (32), 77 (100), 51 (42). HRMS (ESI$^+$): calcd. for $C_{20}H_{15}N_8O_2^+$ 399.13187; found 399.1321.

3-[5-Amino-1-(4-methoxyphenyl)-1*H*-pyrazol-4-ylcarbonyl]-7-(4-methoxyphenyl)-3,7-dihydro-4*H*-pyrazolo[3,4-*d*][1,2,3]triazin-4-one (5c): This compound was obtained as a yellow solid in 46 % yield (52 mg). M.p. 190.5 °C (decomp.). ^{1}H NMR [400 MHz, $(CD_3)_2SO$, 25 °C]: δ = 8.72 (s, 1 H, 3-H), 7.95 (d, *J* = 9.0 Hz, 2 H, 8-H, 12-H), 7.73 (s, 1 H, 3′-H), 7.47 (d, *J* = 8.9 Hz, 2 H, 8′-H, 12′-H), 7.23 (d, *J* = 9.1 Hz, 2 H, 9′-H, 11′-H), 7.18 (br. s, 2 H, 5′-H), 7.11 (d, *J* = 8.9 Hz, 2 H, 9-H, 11-H), 3.87 (s, 3 H, 13-H), 3.83 (s, 3 H, 13′-H) ppm. ^{13}C NMR [100 MHz, $(CD_3)_2SO$ 25 °C]: δ = 162.0 (C-6′), 159.3 (C-10), 159.1 (C-10′), 152.1 (C-5′), 152.0 (C-4), 147.2 (C-7a), 141.8 (C-3′), 135.8 (C-3), 130.3 (C-7′), 129.7 (C-14), 126.4 (C-8′, C-12′), 124.7 (C-8, C-12), 114.8 (C-9, C-11, C-9′, C-11′), 107.7 (C-3a), 99.1 (C-4′), 55.6 (C-13), 55.5 (C-13′) ppm. MS (EI): *m/z* (%) = 430 (58), 388 (7), 243 (60), 216 (77), 215 (100), 206 (19), 199 (18), 185 (10), 172 (17), 132 (16), 120 (36), 106 (33), 93 (30), 76 (61), 63 (62), 51 (70), 43 (83). HRMS (ESI$^+$): calcd. for $C_{22}H_{19}N_8O_4^+$ 459.1529; found 459.1529.

3-[5-Amino-1-(4-fluorophenyl)-1*H*-pyrazol-4-ylcarbonyl]-7-(4-fluorophenyl)-3,7-dihydro-4*H*-pyrazolo[3,4-*d*][1,2,3]triazin-4-one (5d): This compound was obtained as a yellow solid in 62 % yield (67 mg). M.p. 182.2 °C (decomp.). ^{1}H NMR [400 MHz, $(CD_3)_2SO$, 25 °C]: δ = 8.76 (s, 1 H, 3-H), 8.13–8.09 (m, 2 H, 8-H, 12-H), 7.75 (s, 1 H, 3′-H), 7.63–7.59 (m, 2 H, 8′-H, 12′-H), 7.54 (br. t, 2 H, *J* = 8.8 Hz, 9-H, 11-H), 7.41 (br. t, 2 H, *J* = 8.8 Hz, 9′-H, 11′-H), 7.34 (br. s, 2 H, 5′-H) ppm. ^{13}C NMR [100 MHz, $(CD_3)_2SO$, 25 °C]: δ = 161.8 (C-6′), 161.6 (*J* = 246.3 Hz, C-10), 161.5 (*J* = 245.4 Hz, C-10′), 152.2 (C-5′), 152.1 (C-4), 147.5 (C-7a), 142.2 (C-3′), 136.2 (C-3), 133.7 (*J* = 2.9 Hz, C-13), 133.3 (*J* = 2.8 Hz, C-13′), 127.2 (*J* = 9.1 Hz, C-8′, C-12′), 125.3 (*J* = 8.9 Hz, C-8, C-12), 116.6 (*J* = 23.3 Hz, C-9, C-11), 116.5 (*J* = 23.1 Hz, C-9′, C-11′), 108.1 (C-3a), 99.2 (C-4′) ppm. MS (EI): *m/z* (%) = 434 (2) [M]$^+$, 433 (2), 405, (10), 363 (4), 231 (20), 204 (41), 174 (6), 149 (7), 132 (7), 121 (13), 109 (37), 95 (100), 75 (52), 52 (33). HRMS (ESI$^+$): calcd. for $C_20H_{12}N_8O_2F_2Na^+$ 457.0949; found 457.0949.

3-[5-Amino-1-(3-fluorophenyl)-1*H*-pyrazol-4-ylcarbonyl]-7-(3-fluorophenyl)-3,7-dihydro-4*H*-pyrazolo[3,4-*d*][1,2,3]triazin-4-one (5e): This compound was obtained as a yellow solid in 51 % yield (55 mg). M.p. 148.3 °C (decomp.). ^{1}H NMR [400 MHz, $(CD_3)_2CO$, 25 °C]: δ = 8.80 (s, 1 H, 3-H), 8.05–7.97 (m, 2 H, 8-H, 12-H), 7.80 (s, 1 H, 3′-H), 7.77–7.67 (m, 1 H, 11-H), 7.64–7.59 (m, 1 H, 11′-H), 7.48–7.31 (m, 6 H, 10-H, 5′-H, 8′-H, 10′-H, 12′-H) ppm. ^{13}C NMR [101 MHz, $(CD_3)_2CO$, 25 °C]: δ = 162.1 (d, *J* = 244.9 Hz, C-9, C-9′), 161.7 (C-6′), 152.1 (C-5′), 151.9 (C-4), 147.7 (C-7a), 142.5 (C-3′), 138.5 (d, *J* = 10.1 Hz, C-13), 138.3 (d, *J* = 10.5 Hz, C-13′), 136.6 (C-3), 131.6 (d, *J* = 9.0 Hz, C-11), 131.3 (d, *J* = 9.2 Hz, C-11′), 120.4 (d, *J* = 2.5 Hz, C-12′), 118.6 (d, *J* = 2.6 Hz, C-12), 115.4 (d, *J* = 21.0 Hz, C-10), 115.1 (d, *J* = 20.9 Hz, C-10′), 111.8 (d, *J* = 24.6 Hz, C-8′), 109.9 (d, *J* = 26.7 Hz, C-8), 108.5 (C-3a), 99.2 (C-4′) ppm. HRMS (ESI$^+$): calcd. for $C_{20}H_{13}N_8O_2F_2^+$ 435.11240; found 435.11201.

3-[5-Amino-1-(2-fluorophenyl)-1*H*-pyrazol-4-ylcarbonyl]-7-(2-fluorophenyl)-3,7-dihydro-4*H*-pyrazolo[3,4-*d*][1,2,3]triazin-4-one (5f): This compound was obtained as a white solid in 66 % yield (71 mg). M.p. 193.4 °C (decomp.). ^{1}H NMR [400 MHz, $(CD_3)_2SO$, 25 °C]: δ = 8.82 (s, 1 H, 3-H), 7.85 (td, *J* = 7.8, 1.6 Hz, 1 H, 11′-H), 7.80 (s, 1 H, 3′-H), 7.76–7.70 (m, 1 H, 12′-H), 7.67–7.64 (m, 1 H, 9′-H), 7.62–7.58 (m, 2 H, 11-H, 12-H), 7.55–7.46 (m, 2 H, 9-H, 10′-H), 7.44 (br. s, 2 H, 5′-H), 7.41–7.37 (m, 1 H, 10-H) ppm. ^{13}C NMR [100 MHz, $(CD_3)_2SO$, 25 °C]: δ = 161.6 (C-6′), 157.0 (*J* = 251.1 Hz, C-8), 155.9 (*J* = 252.6 Hz, C-8′), 153.4 (C-5′), 152.0 (C-4), 148.5 (C-7a), 142.6 (C-3′), 136.9 (C-3), 132.3 (*J* = 7.8 Hz, C-12′), 131.6 (*J* = 7.8 Hz, C-12), 129.4 (C-11), 128.9 (C-11′), 125.5 (*J* = 3.9 Hz, C-10′), 125.4 (*J* = 3.9 Hz, C-10), 124.3 (*J* = 13.4 Hz, C-13), 124.2 (*J* = 11.7 Hz, C-7′), 117.2 (*J* = 19.0 Hz, C-9′), 117.1 (*J* = 18.9 Hz, C-9), 107.6 (C-3a), 98.3 (C-4′) ppm. MS (EI): *m/z* (%) = 435 (9) [M + 1]$^+$, 434 (9) [M]$^+$, 407 (19), 406 (18), 365 (10), 364 (10), 231 (19), 204 (100), 184 (30), 161 (14), 149 (12), 137 (19), 123 (21), 109 (39), 95 (91), 75 (44), 52 (23). HRMS (ESI$^+$): calcd. for $C_{20}H_{12}N_8O_2F_2Na^+$ 457.0949; found 457.0943.

Synthesis of 5-Amino-1-phenyl-1*H*-pyrazole-4-carboxylic Acid (11)

Method 1: Pyrazolotriazinone **4b** (0.051 g, 0.24 mmol) was treated $SOCl_2$ (3 mL) and catalytic amounts of DMF at reflux for 2 h. After that time, the mixture was evaporated under reduced pressure and the resultant solid was washed three times with dichloromethane (15 mL) to facilitate the elimination of remaining $SOCl_2$. The solid was purified by column chromatography using CH_2Cl_2/PhMe/MeOH (8:1:1) as eluent to give **11** (52 %) as a yellow solid. ^{1}H NMR [400 MHz, $(CD_3)_2SO$, 25 °C]: δ = 6.28 (br. s, 2 H), 7,39–7.43 (m, 1 H), 7,51–7.56 (m, 4 H), 7.68 (s, 1 H), 12.07 (br. s, 1 H) ppm. ^{13}C NMR [100 MHz, $(CD_3)_2SO$]: δ = 95,30, 123,44, 127,38, 129,43, 137,99, 140,51, 149,86, 165.26 ppm. MS (EI): *m/z* (%) = 204 (68) $[M + 1]^+$, 203 (79) $[M]^+$, 185 (96), 184 (84), 156 (21), 130 (7), 119 (7), 103 (12), 91 (57), 77 (100), 65 (18), 54 (20), 53 (61), 52 (54), 41 (20).

Method 2: A mixture of **4b** (0.047 g, 0.22 mmol), benzene (7.2 mL), and water (0.8 mL) was heated at reflux for 6 h. The mixture was then cooled and a white solid was obtained that was filtered and submitted to analysis. This solid was identified as 1-phenyl-1*H*-pyrazol-5-amine (**12**) and all the spectral data correspond to those reported in the literature.[27] The aqueous organic mixture recovered from filtration was separated and the organic phase was dried ($MgSO_4$), filtered, and the filtrate evaporated under reduced pressure to give a yellow solid. This solid was then redissolved in acetone and analyzed by GC–MS. The analysis showed the presence of **11** (63 % yield) as the main product and traces of **12** (11 % yield).

Synthesis of 5-Amino-1-phenyl-*N*-(*p*-tolyl)-1*H*-pyrazole-4-carboxamide (13): Benzene (4 mL) was added to a mixture of pyrazolotriazine **4b** (0.023 g, 0.11 mmol) and *p*-toluidine (0.027 g, 0.25 mmol), heated at reflux with stirring for 5 h. The solution was cooled to room temperature and maintained at this temperature for 24 h during which time a white solid formed. The precipitate was then filtered off, washed with cold water, and dried to give **13** (19 mg, 59 % yield) as a yellow solid. ^{1}H NMR [400 MHz, $(CD_3)_2CO$, 25 °C]: δ = 8.91 (s, 1 H, 14-H), 8.01 (s, 1 H, 3-H), 7.64–7.62 (m, 4 H, 9-H, 13-H, 16-H, 20-H), 7.54 (br. t, *J* = 7.9 Hz, 2 H, 10-H, 12-H), 7.40 (br. t, *J* = 7.4 Hz, 1 H, 11-H), 7.12 (d, *J* = 8.2 Hz, 2 H, 17-H, 19-H), 6.30 (br. s, 2 H, 6-H), 2.28 (s, 3 H, 21-H) ppm. ^{13}C NMR [101 MHz, $(CD_3)_2CO$, 25 °C]: δ = 163.9 (C-7), 150.8 (C-5), 139.5 (C-8), 138.7 (C-3), 138.0 (C-15), 133.1 (C-18*), 133.1 (C-18*), 130.3 (C-10, C-12), 129.9 (C-17, C-19), 128.2 (C-11), 124.3 (C-9, C-13), 120.8 (C-16*, C-20*), 120.7 (C-16*, C-20*), 98.9 (determined by HMBC correlation, C-4), 20.8 (C-21) ppm. *Mixture of interconverting rotational isomers with respect to the amide bond. FTIR (KBr): $\tilde{\nu}$ = 3464.60–3313.64 (νN–H), 1642.15 (νC=O amide) cm^{-1}.

Synthesis of 5-Amino-*N*-(4-cyano-1-phenyl-1*H*-pyrazol-5-yl)-1-phenyl-1*H*-pyrazole-4-carboxamide (14): A mixture of pyrazolotriazinone **4b** (0.107 g, 0.50 mmol) and 5-amino-1-phenyl-1*H*-pyrazole-4-carbonitrile (**3b**; 0.092 g, 0.50 mmol) in benzene (15 mL) was heated at reflux for 3 h. After that time, the solvent was evaporated and the solid residue was purified by column chromatography (dichloromethane/ethyl acetate, 9:1) to give **14** as a yellow solid (109 mg, 59 % yield). ^{1}H NMR [400 MHz, $(CD_3)_2SO$, 25 °C]: δ = 6.50 (br. s, 2 H, 6-H), 7.38–7.49 (m, 2 H), 7.52–7.60 (m, 8 H), 8.00 (s, 1 H, 3′-H), 8.34 (s, 1 H, 3-H), 10.32 (br. s, 1 H, 6′-H) ppm. ^{13}C NMR [100 MHz, $(CD_3)_2SO$]: δ = 90.8 (C-4′), 96 (C-4), 113.0 (C-7′), 123.6 (C-9, C-13, C-9′, C-13′), 123.7 (C-9, C-13, C-9′, C-13′), 127.6 (C-11′), 128.8 (C-11), 129.5 (C-10, C-12, C-10′, C-12′), 129.6 (C-10, C-12, C-10′, C-12′), 137.6 (C-8), 137.7 (C-8′), 138.7 (C-5), 141.2 (C-5′), 142.4 (C-3), 150.1 (C-3′), 162.6 (C-7) ppm. MS (EI): *m/z* (%) = 369 (2) $[M]^+$, 368 (2) $[M - 1]^+$, 206 (2), 186 (100), 131 (10), 77 (54), 51 (24).

Computational Procedure: The potential energy surfaces were explored by using the Gaussian 09 package for the DFT calculations.[30] All the relevant stationary points along the main paths, reactants, TSs, intermediates, and products, were fully calculated by using the range-separated correction of the B3LYP functional, CAM-B3LYP (CAM, Coulomb Attenuating Method), with the 6-311+G(d,p) basis set.[31] The obtained stationary points were characterized by Hessian diagonalization and further harmonic frequency analyses to obtain zero-point and thermal corrections for the energies, enthalpies, and free energies. In relevant cases, intrinsic reaction coordinate (IRC) simulations were started from the TS-computed modes by using mass-weighted coordinates and maximum step sizes ranging from 0.014 to 0.045 atomic units.[22] A summary of IRC simulations for most cases are included in Figures S7–S16 in the Supporting Information, showing the electronic energies (relative to the TS energy) against the range of intrinsic reaction coordinate explored and the 3D structures of intermediates and TSs. All optimizations and frequency analyses were performed within the IEFPCM model for benzene,[32] the solvent used in the synthesis of **5b**,**c** starting from **4b**,**c**. In the case of the mechanism for the **4b** → **5b** reaction, the structures of all the stationary points found were also subjected to single-point energy calculations at the MP2, MP3, and MP4(DQ)/6-311+G(d,p) levels of theory,[33] also within the IEFPCM model for benzene as solvent. The results are summarized in Table S2. The free-energy profiles obtained at the MP2, MP3, MP4, and CAM-B3LYP levels of theory are superimposed for each of the individual paths A–E in Figure S6, and generally show good agreement between the DFT and MP4 ab initio results. Visualization and graphics rendering were carried out with Molden and VMD 1.8.9.[34] The relative free energies reported in Scheme 4 were obtained by taking the standard free energies from the normal analysis of reactants **4b** and **4c** as reference, that is, 2 equivalents of the reactants as zero. The electronic energies in Hartrees, zero-point energies, and thermal corrections are available in Table S1 in the Supporting Information, as well as the whole set of Cartesian coordinates for all the stationary points (Part 3 in the Supporting Information).

Acknowledgments

This work was supported by SECYT-UNC together with the National Research Council of Argentina (CONICET). M. L. S. acknowledges the receipt of a scholarship from the CONICET. The authors also thank Dr. Novruz Akhmedov (West Virginia University, USA) for his valuable contribution in the structural elucidation of the pyrazolotriazine compounds.

Keywords: Nitrogen heterocycles · Nitrogen extrusion · Ketenes · Density functional calculations · Diazotization · Reaction mechanisms

[1] a) P. C. Srivastava, R. K. Robins, R. B. Meyer Jr. in *Chemistry of Nucleosides and Nucleotides, Vol. 1* (Ed.: L. B. Townsend), Plenum Press, New York, **1988**, pp. 113–281; b) H. Rosemeyer, *Chem. Biodiversity* **2004**, *1*, 361–401; c) I. Novosjolova, E. Bizdena, M. Turks, *Eur. J. Org. Chem.* **2015**, *2015*, 3629–3649; d) M. Chauhan, R. Kumar, *Med. Chem. Res.* **2015**, *24*, 2259–2282.

[2] S. Krawczyk, M. Migawa, J. Drach, L. Townsend, *Nucleosides Nucleotides Nucleic Acids* **2000**, *19*, 39–68.

[3] M. Long, W. Parker, *Biochem. Pharmacol.* **2006**, *71*, 1671–1682.

[4] J. Kelley, D. Wilson, V. Styles, F. Soroko, B. Cooper, *J. Heterocycl. Chem.* **1995**, *32*, 1417–1421.

[5] E. Moyano, J. Colomer, G. Yranzo, *Eur. J. Org. Chem.* **2008**, 3377–3381.

[6] J. Colomer, E. Moyano, *Tetrahedron Lett.* **2011**, *52*, 1561–1565.
[7] M. Migawa, L. Townsend, *J. Org. Chem.* **2001**, *66*, 4776–4782.
[8] A. Gurenko, B. Khutova, S. Klyuchko, A. Vasilenko, V. Brovarets, *Chem. Heterocycl. Compd.* **2014**, *50*, 528–536.
[9] M. Migawa, L. Townsend, *Org. Lett.* **1999**, *1*, 537–539.
[10] N. Peet, *J. Heterocycl. Chem.* **1986**, *23*, 193–197.
[11] B. Khutova, S. Klyuchko, A. Gurenko, A. Vasilenko, A. Balya, E. Rusanov, V. Brovarets, *Chem. Heterocycl. Compd.* **2012**, *48*, 1251–1261.
[12] B. Khutova, S. Klyuchko, A. Gurenko, A. Vasilenko, E. Rusanov, V. Brovarets, *Chem. Heterocycl. Compd.* **2013**, *49*, 922–929.
[13] C. J. Smith, F. J. Iglesias-Sigüenza, I. R. Baxendale, S. V. Ley, *Org. Biomol. Chem.* **2007**, *5*, 2758–2761.
[14] I. Ledenyova, V. Didenko, Kh. Shikhaliev, *Chem. Het. Compd.* **2014**, *50*, 1214–1243.
[15] A. Murray, K. Vaughan, *J. Chem. Soc., C* **1970**, 2070–2074.
[16] G. Baig, M. F. G. Stevens, K. J. Vaughan, *J. Chem. Soc., Perkin Trans. 1* **1984**, 999–1003.
[17] M. Ménager, X. Pan, P. Wong-Wah-Chung, M. Sarakha, *J. Photochem. Photobiol. A* **2007**, *192*, 41–48.
[18] R. Smalley, H. Suschitzky, E. Tanner, *Tetrahedron Lett.* **1966**, *7*, 3465–3469.
[19] D. Hey, C. Rees, A. Todd, *J. Chem. Soc., C* **1968**, 1028–1029.
[20] J. Archer, A. Barker, R. Smalley, *J. Chem. Soc., Perkin Trans. 1* **1973**, 1169–1173.
[21] S. Chiu, C. Chou, *Tetrahedron Lett.* **1999**, *40*, 9271–9272.
[22] I. Malvacio, E. Moyano, D. Vera, *RSC Adv.* **2016**, *6*, 83973–88981.
[23] R. Vander Meer, R. Olofson, *J. Org. Chem.* **1984**, *49*, 3373–3377.
[24] M. Siddiqui, M. Stevens, *J. Chem. Soc., Perkin Trans. 1* **1974**, 2482–2486.
[25] L. George, P. Bernhardt, K.-P. Netsch, C. Wentrup, *Org. Biomol. Chem.* **2004**, *2*, 3518–3526.
[26] O. O. Brovarets', R. O. Zhurakivsky, D. M. Hovorun, *Chem. Phys. Lett.* **2014**, *592*, 247–255.
[27] O. O. Brovarets', R. O. Zhurakivsky, D. M. Hovorun, *J. Biomol. Struct. Dyn.* **2015**, *33*, 674–689.
[28] G. Ege, H. Franz, *J. Heterocycl. Chem.* **1982**, *19*, 1267–1273.
[29] J. Li, Y. Zhao, X. L. Zhao, X. Y. Yuan, P. Gong, *Arch. Pharm. (Weinheim)* **2006**, *339*, 593–597.
[30] M. J. Frisch, G. W. Trucks, H. B. Schlegel, G. E. Scuseria, M. A. Robb, J. R. Cheeseman, G. Scalmani, V. Barone, B. Mennucci, G. A. Petersson, H. Nakatsuji, M. Caricato, X. Li, H. P. Hratchian, A. F. Izmaylov, J. Bloino, G. Zheng, J. L. Sonnenberg, M. Hada, M. Ehara, K. Toyota, R. Fukuda, J. Hasegawa, M. Ishida, T. Nakajima, Y. Honda, O. Kitao, H. Nakai, T. Vreven, J. A. Montgomery Jr., J. E. Peralta, F. Ogliaro, M. Bearpark, J. J. Heyd, E. Brothers, K. N. Kudin, V. N. Staroverov, R. Kobayashi, J. Normand, K. Raghavachari, A. Rendell, J. C. Burant, S. S. Iyengar, J. Tomasi, M. Cossi, N. Rega, J. M. Millam, M. Klene, J. E. Knox, J. B. Cross, V. Bakken, C. Adamo, J. Jaramillo, R. Gomperts, R. E. Stratmann, O. Yazyev, A. J. Austin, R. Cammi, C. Pomelli, J. W. Ochterski, R. L. Martin, K. Morokuma, V. G. Zakrzewski, G. A. Voth, P. Salvador, J. J. Dannenberg, S. Dapprich, A. D. Daniels, Ö. Farkas, J. B. Foresman, J. V. Ortiz, J. Cioslowski, D. J. Fox, *Gaussian 09, Revision E.01*, Gaussian, Inc., Wallingford CT, **2009**.
[31] T. Yanai, D. P. Tew, N. C. Handy, *Chem. Phys. Lett.* **2004**, *393*, 51–57.
[32] G. Scalmani, M. J. Frisch, *J. Chem. Phys.* **2010**, *132*, 114110–114115.
[33] K. Raghavachari, M. J. Frisch, J. A. Pople, *J. Chem. Phys.* **1980**, *72*, 4244–4245.
[34] *Visual Molecular Dynamics (VMD), version 1.8.9*, http://www.ks.uiuc.edu/Research/vmd.

Received: November 4, 2017

